Using high-resolution multibeam bathymetry to identify seafloor surface rupture along the Palos Verdes fault complex in offshore southern California

M.S. Marlow
J.V. Gardner
W.R. Normark
U.S. Geological Survey, 345 Middlefield Road, Menlo Park, California 94025, USA

ABSTRACT

Recently acquired high-resolution multibeam bathymetric data reveal several linear traces that are the surficial expressions of seafloor rupture of Holocene faults on the upper continental slope southeast of the Palos Verdes Peninsula. High-resolution multichannel and boomer seismic-reflection profiles show that these linear ruptures are the surficial expressions of Holocene faults with vertical to steep dips. The most prominent fault on the multibeam bathymetry is about 10 km to the west of the mapped trace of the Palos Verdes fault and extends for at least 14 km between the shelf edge and the base of the continental slope. This fault is informally called the Avalon Knoll fault for the nearby geographic feature of that name. Seismic-reflection profiles show that the Avalon Knoll fault is part of a northwest-trending complex of faults and anticlinal uplifts that are evident as scarps and bathymetric highs on the multibeam bathymetry. This fault complex may extend onshore and contribute to the missing balance of Quaternary uplift determined for the Palos Verdes Hills and not accounted for by vertical uplift along the onshore Palos Verdes fault. We investigate the extent of the newly located offshore Avalon Knoll fault and use this mapped fault length to estimate likely minimum magnitudes for events along this fault.

Keywords: tectonics, faulting, imagery, Palos Verdes Peninsula.

INTRODUCTION

Geologic Setting

The Palos Verdes Peninsula (Figs. 1 and 2) is dominated by the Palos Verdes Hills, the topographic expression of a doubly plunging anticlinorium that is currently active (Ward and Valensise, 1994). Uplift and anticlinal growth of the peninsula have been linked in part with activity of the northwest-trending, southwest-dipping Palos Verdes fault (Fig. 1; Woodring et al., 1946; Yerkes et al., 1965; Ward and Valensise, 1994). However, a study by Clarke et al. (1998) in the inner Los Angeles Harbor suggests that only about 20%–30% of this uplift during late Pleistocene and Holocene time (Ponti and Lajoie, 1992) can be attributed directly to the vertical component of Palos Verdes fault displacement. This finding implies that another, as yet unlocated, fault (or faults) is a major contributor to the balance of late Quaternary uplift determined for the Palos Verdes Hills.

The Palos Verdes fault is divisible into southern, central, and northern segments (Fig. 1; Ward and Valensise, 1994). The northern segment underlies Santa Monica Bay. The central segment, about 20 km long, is located onshore adjacent to the Palos Verdes Hills. The southern segment extends offshore beneath San Pedro Bay, and this segment may bifurcate below the shelf edge into two fault strands that trend southeastward to Lasuen Knoll (Fig. 1; Vedder et al., 1986; Clarke et al., 1987, 1998; Clarke and Kennedy, 1998).

Offshore geophysical investigations suggest that there is significant right-lateral offset along the Palos Verdes fault, as evidenced by abrupt changes both in the configuration of the basement rocks (Catalina Schist) and in the lithology and thickness of overlying sedimentary units (Greene et al., 1975; Darrow and Fischer, 1983; Clarke et al., 1983, 1985; Ward and Valensise, 1994; Petersen and Wesnousky, 1994). Gravity data (McCulloh, 1960) and seismic-reflection profiles (Nardin and Henyey, 1978; Stephenson et al., 1992) suggest that the geometry of the Palos Verdes fault involves a left-stepping, restraining bend that is responsible for significant changes in strike at the southern and central segment boundaries and for growth of the Palos Verdes Hills anticline (Ward and Valensise, 1994). In this paper we use high-resolution multibeam bathymetry (Dartnell and Gardner, 1999) and newly acquired seismic-reflection profiles to investigate the offshore complexity of the Palos Verdes fault beneath the continental slope southeast of San Pedro Bay (Fig. 2).

Equipment

The multibeam bathymetry data were collected by using three high-resolution multibeam systems (Kongsberg Simrad EM300, EM950, and EM3000D), each differing in frequency, number of beams, and beam angles (Dartnell and Gardner, 1999). Each of the systems provides spatial accuracy of better than 1 m and depth accuracy that varies from about 10 cm on the shelf to about 100 cm at 800 m water depth. Data from the three surveys were collated at a uniform 16 m grid spacing for the overview of Figure 2, but subareas were processed at the highest reso-

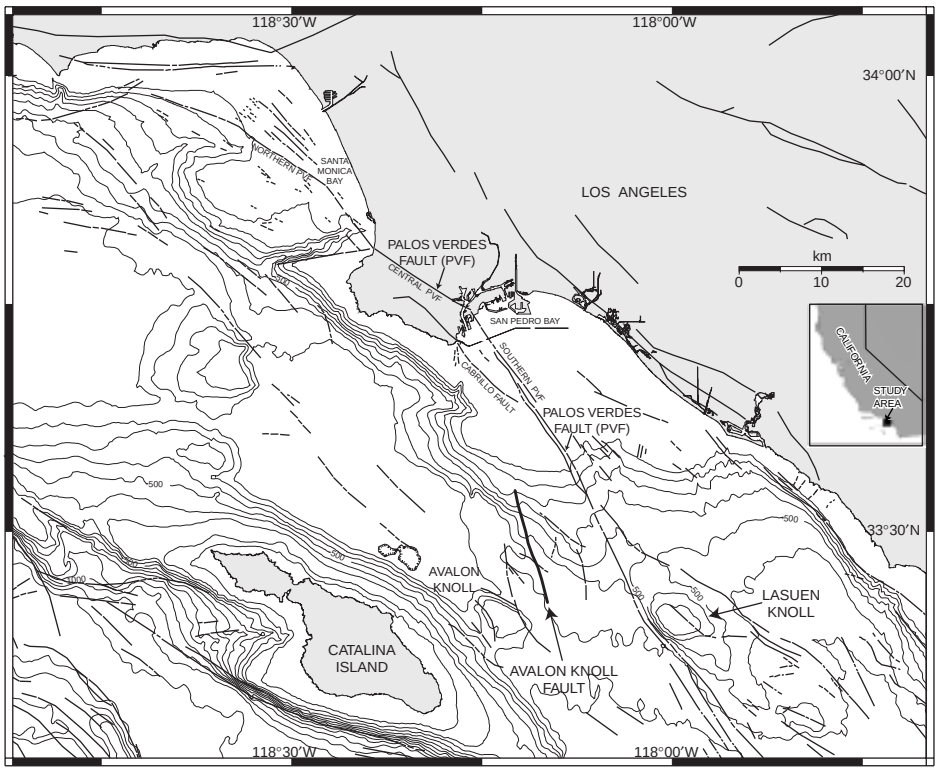

Figure 1. Bathymetry and major onshore (Jennings, 1994) and offshore (Greene and Kennedy, 1987) faults of central southern California. Avalon Knoll fault (heavy line) is from this study. Bathymetry is from Smith and Sandwell (1997).

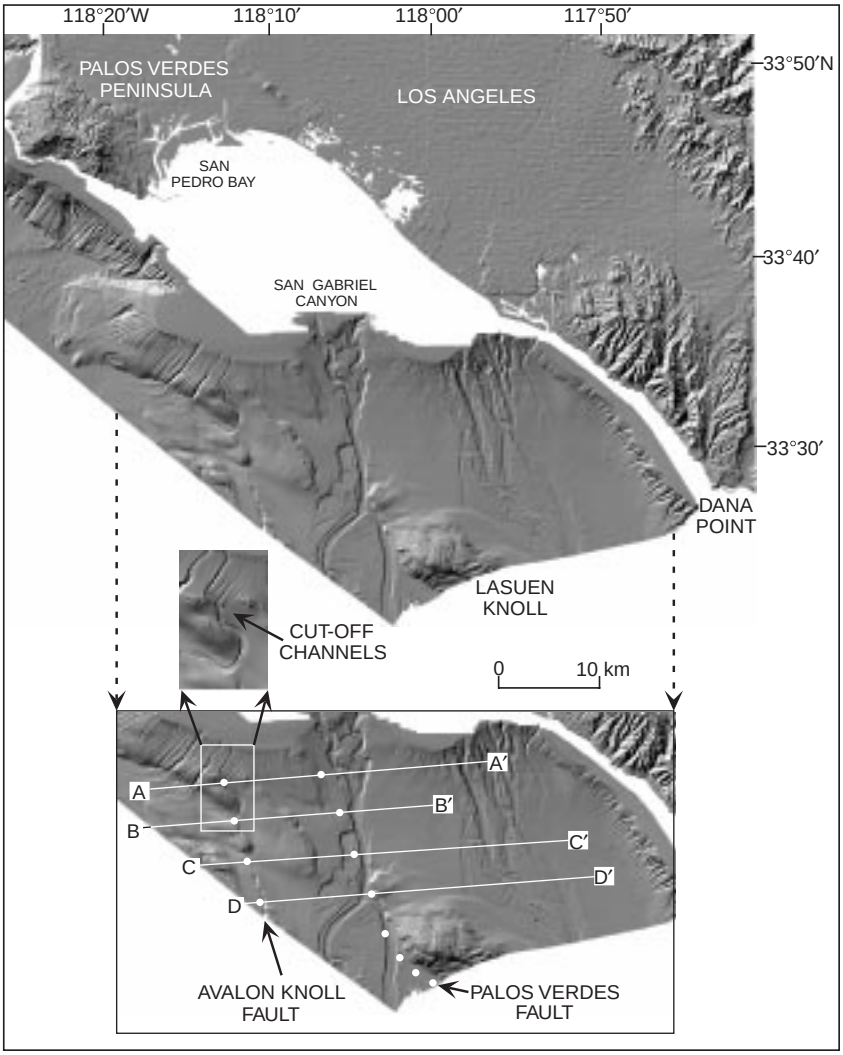

Figure 2. Shaded-relief map of central southern California (Dartnell and Gardner, 1999). Inset shows location of seismic-reflection profiles in Figures 3 and 4, and enlarged detail image shows cutoff drainage channels. Shaded-relief map was generated by using Lambertian model with illumination of 45° elevation and azimuth of 315°.

lution allowable by the data. The interpretations in this report are based on the subarea maps, which have resolutions (grid cell sizes) of 2 m on the outer shelf, 4 m on the upper slope, and 8 m on the lower slope and adjacent basin.

The sound source for the multichannel seismic-reflection data was a 35 in^3 (573.5 cm^3) double-chamber, gas-injection gun firing every 12 s at a pressure of ~3000 psi (20 000 kPa). Data were recorded with a 24-channel streamer having 10-m-long groups and 3 geophones per group. The sound source for a Huntec high-resolution seismic-reflection profile was a 350 J boomer plate, and returning signals were received on a 5 m, 10-element hydrophone array.

PALOS VERDES AND AVALON KNOLL FAULTS

The multibeam bathymetry delineates a scarp on the southwestern side of Lasuen Knoll (Fig. 2) that corresponds to the mapped trace of the Palos Verdes fault (Vedder et al., 1986; Clarke et al., 1987). The Palos Verdes fault changes strike along the western flank of Lasuen Knoll and extends to the northwest as a distinct feature of the continental slope slightly west of San Gabriel Canyon (Fig. 2). Seismic-reflection profile D-D′ (Fig. 3) shows that the valley extending from San Gabriel Canyon is adjacent to a prominent scarp above a fault that truncates east-dipping strata underlying Lasuen Knoll. Stratified beds west of the canyon are folded into a series of anticlinal uplifts that can be followed up the continental slope parallel to the Palos Verdes fault (Fig. 3). The seismic-reflection profiles show that the main break of the Palos Verdes fault trends upslope slightly to the west of the main channel of San Gabriel Canyon.

A second fault, located about 10 km west of the Palos Verdes fault, can be traced 14 km up the slope on seismic-reflection profiles (Fig. 3). Multibeam bathymetry shows a series of left-stepping, en echelon scarps that correspond to the fault imaged in the reflection profiles. The alignment of the scarps in the bathymetric data suggests that these breaks are one fault, here named the Avalon Knoll fault after nearby Avalon Knoll just south of the multibeam bathymetry coverage (Figs. 1 and 2). The Avalon Knoll fault is subparallel to the Palos Verdes fault. These two faults and intervening structural blocks form a complex ~10 km wide that trends northwest beneath the continental slope. Folding associated with the Palos Verdes fault varies in intensity and bathymetric expression on either side of the Palos Verdes fault between Lasuen Knoll and the shelf edge, suggesting that scissoring or differential uplift of tectonic blocks has occurred along the fault trace. The Avalon Knoll fault may continue northwest beneath the San Pedro shelf and Palos Verdes Hills. If so, however, the Avalon Knoll fault must be west of the Holocene Cabrillo fault (Fig. 1), which is well located from seismic-reflection data from the Palos Verdes shelf and which does not appear to be cut by other faults (Greene et al., 1975; Clarke et al., 1985; Vedder et al., 1986).

The northern scarp of the Avalon Knoll fault cuts three channels incised into the upper continental slope (see inset in Fig. 2). One of the cut channels is visible on both sides of the scarp, indicating that the scarp is younger than the channel. Drainage in all three channels is diverted by the scarp into a broad, semicircular channel that skirts around a bathymetric high at the base of the upper slope (Fig. 2).

A high-resolution Huntec seismic-reflection profile crosses the southern part of the Avalon Knoll fault, revealing depositional thinning and offsets in the youngest Holocene strata present across the fault and beneath the continental slope (Fig. 4, location shown on D-D′ of Fig. 3; strata age from Vedder et al., 1986). Sedimentary units, which are a minimum of about 30 m (0.04 s two-way time) thick, are uplifted east of the fault scarp. This evidence of recent activity on the Avalon Knoll fault is consistent with the observed truncation of geologically youthful channels by the fault farther up the slope and with the well-preserved linear scarps evident on the multibeam bathymetry (Fig. 2).

EPICENTERS

A map plot of epicenters relocated by Richards-Dinger and Shearer (2000) that covers the period 1975–1998 is shown with the multibeam bathymetry in Figure 5. Three magnitude (Ml) 4 to Ml 5 events are located beneath the continental slope south of San Pedro Bay. These events appear to be spatially associated with the Palos Verdes and Avalon Knoll faults and the deformed anticlinal blocks between these faults. Smaller events are scattered beneath the continental slope west of Lasuen Knoll and beneath the inner shelf in San Pedro Bay. These diffuse zones of seismicity may reflect activity within and beneath the deformed blocks between the two fault zones, as well as activity on other faults in the region. Alternatively, the diffuse zones of seismicity may reflect poor locations because of a lack of offshore receiver stations.

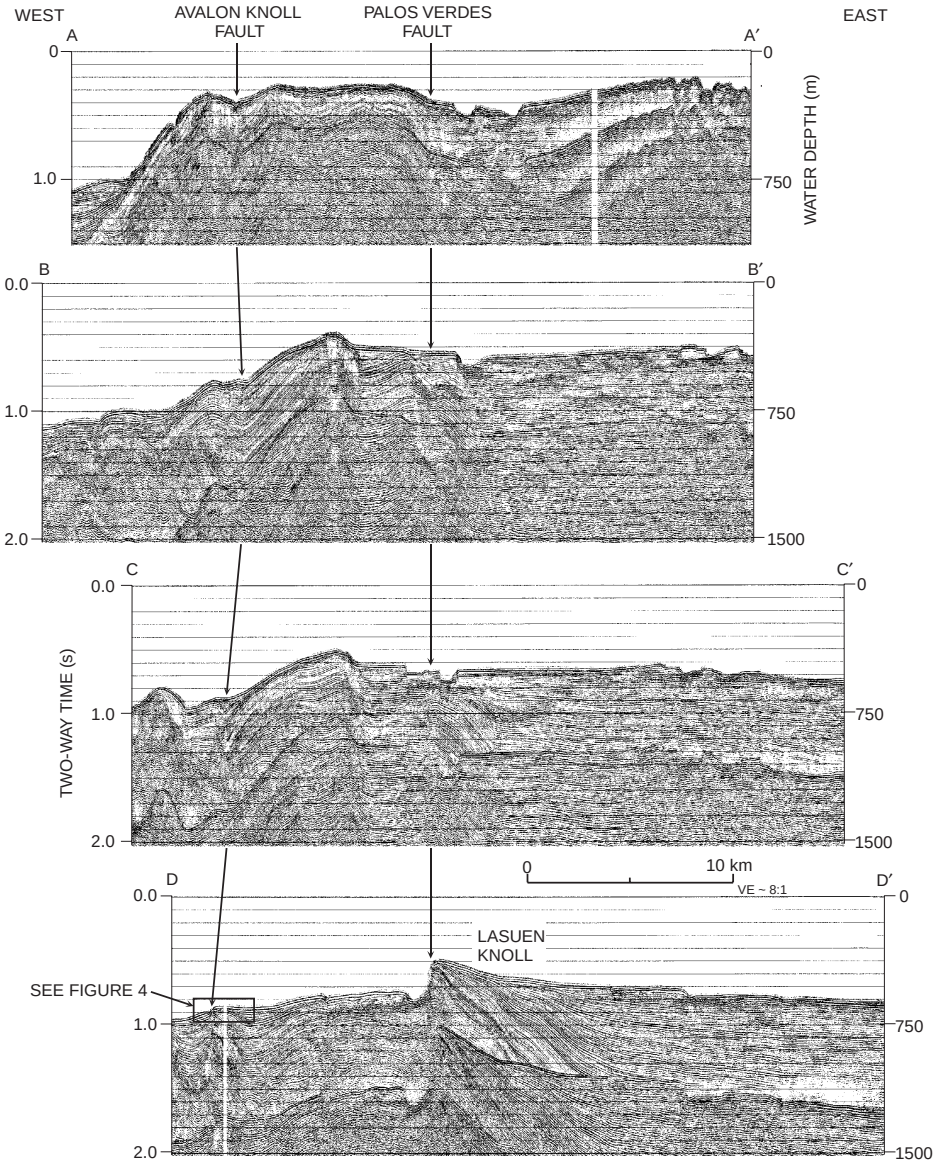

Figure 3. High-resolution, multichannel seismic-reflection profiles across continental slope south of San Pedro Bay. Profiles are aligned along trace of Palos Verdes fault. See Figure 2 for profile locations.

DISCUSSION

Onshore and Offshore Magnitude Estimates

Ward and Valensise (1994) analyzed data from 13 emergent marine terraces in the Palos Verdes Hills (Ponti, 1989; Ponti and Lajoie, 1992) and derived a fault-dislocation model for the onshore segment of the Palos Verdes fault. Their model calls for 3.0–3.7 mm·yr^{-1} of oblique, dextral-reverse slip on a 19-km-long fault striking N128.5°E and dipping 67° to the southwest at 6–12 km depth beneath the Palos Verdes Peninsula. Faulting would have commenced at 3.0–2.4 Ma, and the largest earthquakes on the fault are estimated to have magnitudes of M_w ~6.75 with recurrence intervals of ~2000 yr. Estimated repeat times for $M_w \geq 5$ and $M_w \geq 6$ earthquakes are between 33–59 yr and 330–590 yr, where M_w is the moment magnitude.

McNeilan et al. (1996) used high-resolution seismic-reflection profiles and borehole data from the Los Angeles Outer Harbor to estimate slip rate for the San Pedro shelf segment of the Palos Verdes fault (southern segment, Fig. 1). They estimated the slip rate to be between 2.7 and 3.0 mm/yr for the past 7.8 to 8.0 k.y. By using the slip-rate and segmentation models for the fault, they estimated that the Palos Verdes fault could generate a M_w 7.0–7.2 event about every 400 to 900 yr.

Avalon Knoll Fault Magnitude Estimate

The Avalon Knoll fault exhibits three en echelon breaks in the seafloor that are 2.0, 1.5, and 5.0 km in length (from north to south, Fig. 2). If these three seafloor breaks are surface expressions of a single rupture segment, then the cumulative active fault length is at least 14 km. This is a minimum length because the southern trace extends to the limit of our imagery data, and the northern extent of faulting is uncertain. This minimum fault length is capable of generating a 6.5 magnitude earthquake according to the regression relationship between surface-rupture length and magnitude (M_w) by Wells and Coppersmith (1994; see also Yeats et al., 1997). This is less than but comparable to the estimated magnitude anticipated for the Palos Verdes fault (Ward and Valensise, 1994; McNeilan et al., 1996). The comparatively clear seafloor expression of the Avalon Knoll fault suggests that the last displacement may have been more recent than the southern Palos Verdes fault displacement (Figs. 1 and 2). However, the Avalon Knoll fault may be a strand of either the central or southern Palos Verdes fault.

CONCLUSIONS

Multibeam bathymetry allows the ready identification of a fault trace on the seafloor. The images also show offset slope drainage systems that would not be evident on a grid of geophysical profiles alone. Multibeam bathymetry is a valuable tool for delineating offshore earthquake hazards through delineation of the length and geometry of offshore faults exposed at the seafloor. Faults can be confirmed by carefully sited, high-resolution seismic-reflection profiles. The minimum length of the newly discovered Avalon Knoll fault yields an estimated minimum earthquake magnitude (M_w) of 6.5 for this element of the Palos Verdes fault complex.

ACKNOWLEDGMENTS

We thank S.H. Clarke, S. Hecker, A.C. Hine, and T.M. Niemi for their thoughtful and useful reviews.

REFERENCES CITED

Clarke, S.H., and Kennedy, M.P., 1998, Analysis of late Quaternary faulting in the Los Angeles Harbor area and hazard to the Vincent Thomas Bridge:

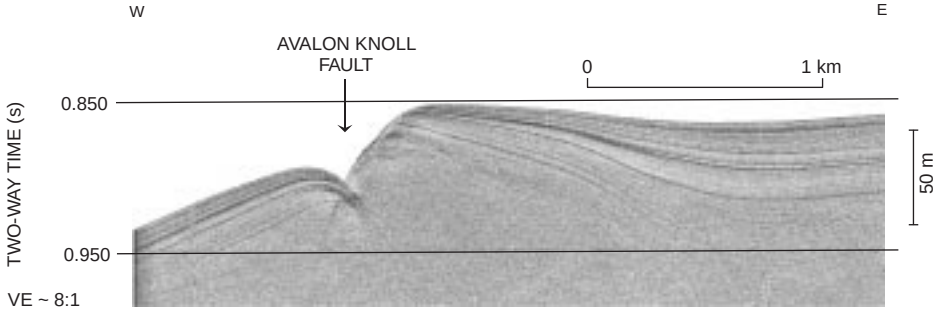

Figure 4. High-resolution Huntec seismic-reflection profile across Avalon Knoll fault. Vertical scale assumes velocity of 1600 m/s. See Figure 3, D-D′, for location of profile.

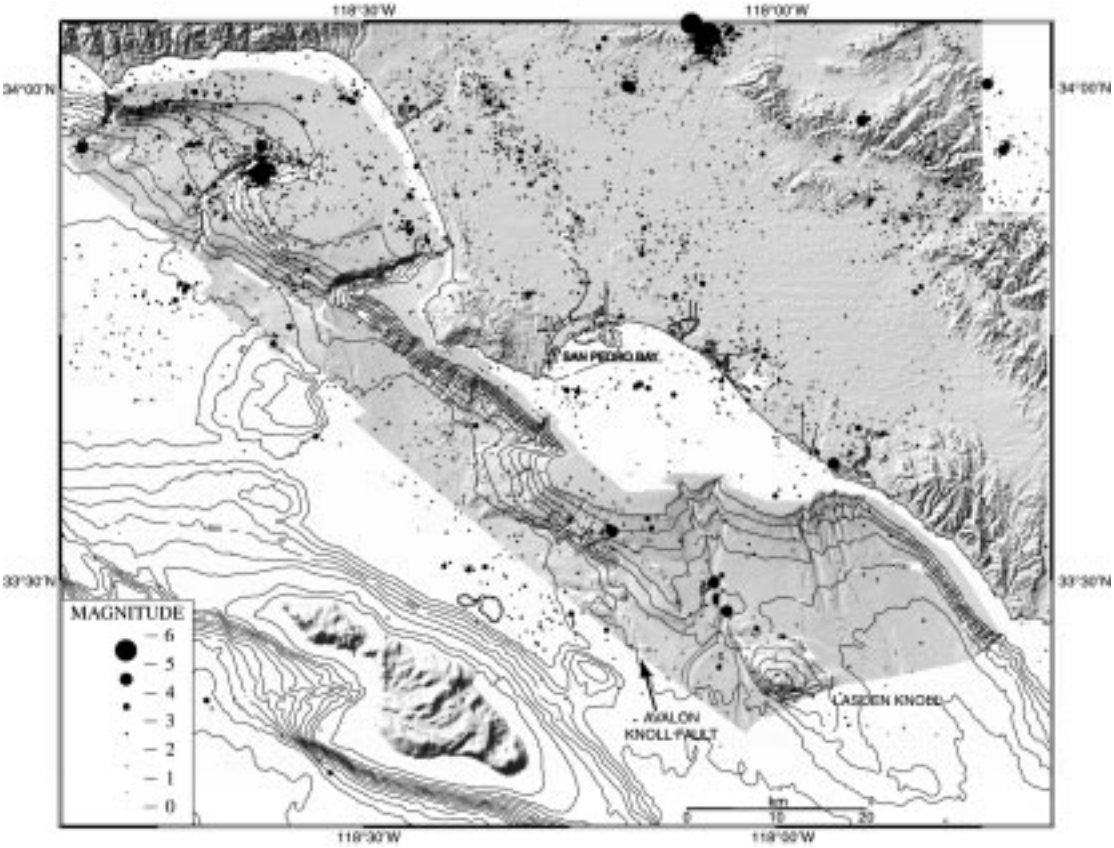

Figure 5. Shaded-relief map of onshore and offshore central southern California showing epicenters from 1975 to 1998 relocated by Richards-Dinger and Shearer (2000). Magnitudes are coda magnitudes (M_c) for events shown and are available from Southern California Earthquake Center Data Center (SCECDC) (http://www.scecdc.scec.org, September 1999).

California Division of Mines and Geology Open-File Report 98-01, 27 p.

Clarke, S.H., Greene, H.G., Field, M.E., and Lee, W.H.K., 1983, Reconnaissance geology and geologic hazards of selected areas of the southern California borderland: U.S. Geological Survey Open-File Report 83-62, 78 p.

Clarke, S.H., Greene, H.G., and Kennedy, M.P., 1985, Identifying potentially active faults and unstable slopes offshore, *in* Ziony, J.I., ed., Evaluating earthquake hazards in the Los Angeles region: An earth-science perspective: U.S. Geological Survey Professional Paper 1360, p. 347–373.

Clarke, S.H., Greene, H.G., Kennedy, M.P., and Vedder, J.G., 1987, Geologic map of the inner-southern California continental margin, *in* Greene, H.G., and Kennedy, M.P., eds., Geology of the inner-southern California continental margin: California Division of Mines and Geology, California Continental Margin Geologic Map Series, Map 1A, scale 1:250 000.

Clarke, S.H., Kennedy, M.P., Ponti, D.J., Moody, C., and Wilson, J., 1998, Kinematics of the Palos Verdes fault zone in Los Angeles Harbor, California, from multidisciplinary studies: Geological Society of America Abstracts with Programs, v. 30, no. 5, p. 9–10.

Darrow, A.C., and Fischer, P.J., 1983, Activity and earthquake potential of the Palos Verdes fault: U.S. Geological Survey Technical Report Contribution 14-08-001-19786, 90 p.

Dartnell, P., and Gardner, J.V., 1999, Seafloor images and data from multibeam surveys in San Francisco Bay, southern California, Hawaii, the Gulf of Mexico, and Lake Tahoe, California-Nevada: U.S. Geological Survey Digital Data Series DDS-55, version 1 (CD-ROM).

Greene, H.G., and Kennedy, M.P., eds., 1987, Geology of the inner-southern California continental margin: California Division of Mines and Geology, California Continental Margin Geologic Map Series, scale 1:250 000.

Greene, H.G., Clarke, S.H., Field, M.E., Linker, F.I., and Wagner, H.C., 1975, Preliminary report on the environmental geology of selected areas of the southern California borderland: U.S. Geological Survey Open-File Report 75-596, 70 p.

Jennings, C.W., 1994, Fault activity map of California and adjacent areas with location and ages of recent volcanic eruptions: California Division of Mines and Geology, California Geologic Data Map Series, map no. 6, scale 1:750 000.

McCulloh, T.H., 1960, Gravity variations and the geology of the Los Angeles basin of California: U.S. Geological Survey Professional Paper 400B, p. 320–325.

McNeilan, T.W., Rockwell, T.K., and Resnick, G.S., 1996, Style and rate of Holocene slip, Palos Verdes fault, southern California: Journal of Geophysical Research, v. 101, p. 8317–8334.

Nardin, T.R., and Henyey, T.L., 1978, Pliocene-Pleistocene diastrophism of Santa Monica and San Pedro shelves, California continental borderland: American Association of Petroleum Geologists Bulletin, v. 62, p. 247–272.

Petersen, M.D., and Wesnousky, S.G., 1994, Fault slip rates and earthquake histories for active faults in southern California: Seismological Society of America Bulletin, v. 84, p. 1608–1649.

Ponti, D.J., 1989, Aminostratigraphy and chronostratigraphy of Pleistocene marine sediments, southwestern Los Angeles basin, California [Ph.D. thesis]: Boulder, University of Colorado, 409 p.

Ponti, D.J., and Lajoie, K.R., 1992, Chronostratigraphic implications of tectonic deformation of Palos Verdes and Signal Hills, Los Angeles basin, California: Proceedings, Annual Meeting, 35th, Association of Engineering Geologists, p. 617–620.

Richards-Dinger, K.B., and Shearer, P.M., 2000, Earthquake locations in southern California obtained using source specific station terms: Journal of Geophysical Research (in press).

Smith, W.H.F., and Sandwell, D.T., 1997, Global seafloor topography from satellite altimetry and ship depth soundings: Science, v. 277, p. 1956–1962.

Stephenson, W.J., Odum, J., Shedlock, K.M., Pratt, T.L., and Williams, R.A., 1992, Mini Sosie high-resolution seismic method aids hazards studies: Eos (Transactions, American Geophysical Union), v. 73, p. 473, 475, 476.

Vedder, J.G., Greene, H.G., Clarke, S.H., and Kennedy, M.P., 1986, Geologic map of the mid-southern California continental margin, *in* Greene, H.G., and Kennedy, M.P., eds., Geology of the inner-southern California continental margin: California Division of Mines and Geology, California Continental Margin Geologic Map Series, Map 2A, scale 1:250 000.

Ward, S.N., and Valensise, G., 1994, The Palos Verdes terraces, California: Bathtub rings from a buried reverse fault: Journal of Geophysical Research, v. 99, p. 4485–4494.

Wells, D.L., and Coppersmith, K.J., 1994, New empirical relationships among magnitude, rupture length, rupture width, rupture area, and surface displacement: Seismological Society of America Bulletin, v. 84, p. 974–1002.

Woodring, W.P., Bramlette, M.N., and Kew, W.S.W., 1946, Geology and paleontology of the Palos Verdes Hills, California: U.S. Geological Survey Professional Paper 207, 145 p.

Yeats, R.S., Sieh, K., and Allen, C.R., 1997, The geology of earthquakes: New York, Oxford University Press, 568 p.

Yerkes, R.F., McCulloh, T.H., Schoelhamer, J.E., and Vedder, J.G., 1965, Geology of the eastern Los Angeles basin, southern California: U.S. Geological Survey Professional Paper 420-A, 57 p.

Manuscript received December 28, 1999
Revised manuscript received March 13, 2000
Manuscript accepted March 29, 2000